Phylogenomics reveals dynamic evolution of fungal nitric oxide reductases and their relationship to secondary metabolism

Running title:

Phylogenomics link *p450nor* to secondary metabolism

***Authors*:**

Steven A. Higgins[1,3], Christopher W. Schadt[1,2,3], Patrick B. Matheny[4], and Frank E. Löffler[1,2,3,5,6,7]*

***Author Affiliations*:**

[1]Department of Microbiology, University of Tennessee, Knoxville, TN, 37996, USA.

[2]University of Tennessee and Oak Ridge National Laboratory (UT-ORNL) Joint Institute for Biological Sciences (JIBS), Oak Ridge, Tennessee, USA.

[3]Biosciences Division, Oak Ridge National Laboratory, Oak Ridge, Tennessee, USA.

[4]Department of Ecology and Evolutionary Biology, University of Tennessee, Knoxville, Tennessee, USA.

[5]Department of Civil and Environmental Engineering, University of Tennessee, Knoxville, Tennessee, USA.

[6]Department of Biosystems Engineering & Soil Science, University of Tennessee, Knoxville, Tennessee, USA.

[7]Center for Environmental Biotechnology, University of Tennessee, Knoxville, Tennessee, USA.

***Correspondence to:**

Frank E. Löffler
706 Science and Engineering Building
1414 Circle Drive
Knoxville, TN 37996-2000
865-974-4933
frank.loeffler@utk.edu

Keywords:
P450nor, fungi, nitrous oxide, secondary metabolism, nitrogen cycle, nitric oxide, horizontal gene transfer

Abstract

Fungi expressing P450nor, an unconventional nitric oxide (NO) reducing cytochrome P450, are thought to be significant contributors to soil nitrous oxide (N_2O) emissions. However, fungal contributions to N_2O emissions remain uncertain due to inconsistencies in measurements of N_2O formation by fungi. Much of the N_2O emitted from antibiotic-amended soil microcosms is attributed to fungal activity, yet fungal isolates examined in pure culture are poor N_2O producers. To assist in reconciling these conflicting observations and produce a benchmark genomic analysis of fungal denitrifiers, genes underlying fungal denitrification were examined in >700 fungal genomes. Of 167 *p450nor*–containing genomes identified, 0, 30, and 48 also harbored the denitrification genes *narG*, *napA* or *nirK*, respectively. Compared to *napA* and *nirK*, *p450nor* was twice as abundant and exhibited two to five-fold more gene duplications, losses, and transfers, indicating a disconnect between *p450nor* presence and denitrification potential. Furthermore, co-occurrence of *p450nor* with genes encoding NO-detoxifying flavohemoglobins (Spearman r = 0.87, $p = 1.6e^{-10}$) confounds hypotheses regarding P450nor's primary role in NO detoxification. Instead, ancestral state reconstruction united P450nor with actinobacterial cytochrome P450s (CYP105) involved in secondary metabolism (SM) and 19 (11 %) *p450nor*-containing genomic regions were predicted to be SM clusters. Another 40 (24 %) genomes harbored genes nearby *p450nor* predicted to encode hallmark SM functions, providing additional contextual evidence linking *p450nor* to SM. These findings underscore the potential physiological implications of widespread *p450nor* gene transfer, support the novel affiliation of *p450nor* with fungal SM, and challenge the hypothesis of *p450nor*'s primary role in denitrification.

Importance

Fungi are considered substantial contributors to emissions of the greenhouse gas N_2O, owing to the nitric oxide reducing potential of an unusual cytochrome P450 (P450nor). Despite these findings, fungi do not satisfy criteria to be classified as respiratory denitrifiers and methodological biases confound fungal contributions to the N_2O budget. Phylogenetic and genomic analyses distanced N_2O-forming fungi from denitrification and supported a new link between P450nor and SM. Hence, N_2O formed by P450nor activity may be artificially induced or a byproduct of SM. Explorations of P450nor's involvement in SM may facilitate the discovery of new compounds with potential applications in agricultural and pharmaceutical industries. Dissociating *p450nor* from denitrification also informs climate change models and directs research towards organisms and processes most relevant to *in situ* N_2O production.

Introduction

Increased human reliance on fixed nitrogen (N) from the Haber-Bosch process to meet the demands of sustaining an expanding global population has contributed to a 20 % increase in atmospheric nitrous oxide (N_2O), a potent greenhouse gas with ozone destruction potential (1, 2). N_2O is primarily formed by denitrifying members of the *Bacteria* and *Archaea* (3), a prevailing view that has been challenged by experiments reporting that abundant soil- and sediment-inhabiting fungi contribute up to 89 % of the total N_2O emitted from these systems (4–6). Notably, fungi cannot convert N_2O to inert N_2 like many denitrifying bacteria (7), suggesting their contributions to greenhouse effects and ozone destruction could be significant. Fungi are considered to be important sources of N_2O emissions from agroecosystems (8, 9), which are predicted to contribute up to two-thirds of the total N_2O emissions by 2030 (10). Studies of

model fungi show that N_2O formation is due to P450nor, a heme-containing cytochrome P450, that catalyzes the two electron reduction of nitric oxide (NO) to N_2O (11–13). N_2O formation by P450nor is thought to occur exclusively in fungi and the *p450nor* gene has been exploited as a distinctive biomarker in molecular assays to study fungal denitrifier diversity and abundance in the environment (14–16).

Despite these observations, the fungal contributions to N_2O emissions remain uncertain. For example, fungi do not satisfy criteria set forth to classify microorganisms as respiratory denitrifiers (17). N_2O-producing fungi in pure culture do not exhibit a balance between the inorganic N inputs and quantities of N_2O formed (18–20) and possess three to six orders of magnitude lower rates of N_2O production compared to denitrifying bacterial isolates under optimal conditions (4). Fungi also fail to generate anoxic growth yields proportional to the quantity of inorganic N reduced in pure culture (6, 21–23), and no significant relationship was detected between fungal denitrification activity and fungal biomass in anoxic soil incubations (24). Above all, partitioning techniques (antibiotic inhibition and isotope site preference) used to estimate fungal and bacterial contributions to N_2O emissions are biased and often lack corroborating evidence in conjunction with their application, suggesting fungal contributions to N_2O emissions are substantially inflated (5, 25–27). For example, antibiotics are often criticized for lacking both generality and specificity, but the expected biases resulting from the exclusive use of antibiotic inhibition techniques to assess fungal contributions to N_2O emissions remain unaccounted for. Bias could be interpreted by concurrently employing culture-independent techniques (i.e., multi-omics approaches); however, these practices are lacking in investigations of fungal denitrification, and the singular use of antibiotics to partition microbial activity casts

doubt on the quantitative value of observations derived from this approach regarding fungal denitrification (25, 26).

The capacity for N_2O-production conferred by *p450nor* in fungi is a uniquely eukaryotic trait, yet previous investigations have hypothesized an actinobacterial origin for *p450nor* based on sequence comparisons (7, 28–30). Of note, *Actinobacteria* are not considered canonical denitrifying bacteria, and only a few reports of their denitrification capacity exist (31–33). Most members of the *Actinobacteria* possess a truncated denitrification pathway or lack a canonical nitric oxide reductase gene (*nor*) (with the exception of *Corynebacterium* and *Propionibacterium*) (32, 33). Hence, members of the Fungi and *Actinobacteria* share an incomplete denitrification pathway with a potentially limited capacity to perform denitrification. Consistent with the horizontal gene transfer (HGT) hypothesis are sequence similarities between fungal P450nor and actinobacterial P450s of the CYP105 family, many of which have been investigated for their contributions to secondary metabolism (SM) (7, 34). Despite these observations, the prevailing hypothesis regarding *p450nor*'s evolution and function was its acquisition from the *Actinobacteria* and subsequent evolution to fill a novel role in denitrification, specifically the reduction of NO to N_2O (7, 29). The hypothesis that *p450nor* was acquired from one or more members of the *Actinobacteria* and retained an ancestral function in SM surprisingly remains unexplored.

Efforts associated with the 1,000 Fungal Genomes and Assembling the Fungal Tree of Life (AFTOL) projects have resulted in a steady rise in genomic sequence data for members of the fungal kingdom (35, 36). These large scale sequencing efforts facilitate comprehensive phylogenomic investigations with the potential to uncover the causes and consequences of the genomic architecture of fungi and assist in directing research efforts. Hence, the overarching

questions this study addresses are I) what is the breadth of denitrification genes across fungal genomes and what are their evolutionary relationships, and II) can phylogenomic analyses reconcile the conflict in fungal contributions to N_2O formation observed in laboratory and environmental settings? Our comparative genomic and phylogenetic analyses identified a disconnect between *p450nor* and denitrification gene presence and supported a role for P450nor in SM rather than denitrification. Importantly, these results provide an explanation for the minor, non-respiratory capacity of fungi to form N_2O, and suggests N_2O is a byproduct of active SM. These findings transform our understanding of the ecological significance and environmental consequences of *p450nor* presence/absence in fungal genomes.

Results

Infrequent co-occurrence among denitrification genes in fungi

Bioinformatic analyses identified homologs of canonical bacterial and fungal denitrification genes (*narG*, *napA*, *norB*, *nirK*, *nosZ*, *p450nor*) in 712 fungal genomes. Of the denitrification gene set investigated, only *narG*, *napA*, *nirK*, and *p450nor* were detected (Fig. 1). Genes encoding the membrane bound respiratory nitrate reductase (*narG*) were detected in only three fungal genomes (0.42 %) and were excluded from further analysis due to their low occurrence. The genes predicted to encode the periplasmic nitrate reductase (NapA) and the copper-containing nitrite reductase (NirK) were detected in 75 (10.5 %) and 82 (11.5 %) of the 712 fungal genomes analyzed, respectively (Fig. 1, Table S1). In contrast, P450nor gene sequences occurred at approximately twice the frequency in 167 (23 %) of the fungal genomes analyzed, supporting the claim that P450nor-mediated N_2O production may be widespread in fungi (Fig. 1) (37). A breakdown of genus- and family-level denitrification gene abundances in fungal

genomes underscores the disparity in presence/absence of denitrification genes in fungi and is available in Supplemental Information (SI) (Dataset S1, Fig. S1).

Our analyses also revealed a low co-occurrence between *p450nor* and additional fungal denitrification pathway markers. Since *p450nor* is regarded as the sole trait encoding N_2O production in fungi, the co-occurrence of multiple denitrification gene markers would be indicative of a capacity for sequential respiratory denitrification, whereas isolated occurrences could be indicative of alternative processes such as detoxification. The three-gene set *narG*/*nirK*/*p450nor* did not co-occur in any of the fungal genomes examined, whereas co-occurrence of the gene set *napA*/*nirK*/*p450nor* was observed in 18 (10.8 %) of 167 *p450nor*-containing fungal genomes. Sets of at least two co-occurring denitrification traits (i.e., *narG*/*p450nor*, *napA*/*p450nor*, and *nirK*/*p450nor*) were found in 0, 18 and 29 % of fungal genomes, respectively. Of the *napA*-containing fungal genomes, 25 (33 %) also contained a *nirK* gene, whereas 30 % of the *nirK*-containing fungal genomes also harbored a *napA* gene. Evolutionary correlation was strongly supported for the gene sets *napA*/*nirK*, *napA*/*p450nor*, and *nirK*/*p450nor*, with average log Bayes Factor values of 31.9 ± 0.60, 12.2 ± 0.11, and 31.3 ± 0.04, respectively. Hence, the genes *napA*, *nirK*, and *p450nor* occur in related fungal taxa, but co-occurrences were infrequent within the individual fungal genomes analyzed.

Evolutionary forces acting upon denitrification traits within fungi

To identify evolutionary forces shaping the observed distribution of denitrification traits within fungi, comparisons between gene and species trees were assessed with phylogenetic tests and parsimony-informed models to quantify evolutionary events. Visual inspection of *p450nor* gene and species trees indicated potential widespread HGT of *p450nor* within fungi, examples of which included HGT of *p450nor* from the phylum Ascomycota to members of the

Basidiomycota and within and among classes of ascomycetes (Fig. S2). Furthermore, the monophyly of five fungal classes containing *p450nor* (Dothideomycetes, Eurotiomycetes, Leotiomycetes, Sordariomycetes, and Tremellomycetes) were not supported by approximately unbiased (AU) tests ($p \leq 0.05$, Table S2), indicative of dynamic evolution of *p450nor* in most fungal lineages. Although co-phylogeny plots are suggestive of HGT, additional analysis using NOTUNG software was performed to model potential gene duplication (GD), gene transfer (GT), and gene loss (GL) events (38). Of the *napA*, *nirK*, and *p450nor* genes analyzed, the *p450nor* phylogenies had the greatest number of predicted GT events, ranging from 4 to 15 GT events despite applying stringent GT costs within NOTUNG software (Table S3). At GT costs below 9, no temporally consistent optimal solutions were reached, suggesting that GD and GL alone are insufficient to describe the evolutionary dynamics of *p450nor* in fungi. Using the same stringent GT costs, the predicted number of GT events detected for *napA* and *nirK* were much lower, and ranged from 1 to 3 and 0 to 1 GT events for each gene, respectively (Table S3). The reduced number of GT events detected in *napA* and *nirK* phylogenies were also apparent from co-phylogeny plots of each gene (Fig. S3, S4) compared to co-phylogenetic plots for *p450nor* (Fig. S2). Although GT events detected for *napA* were lower than *p450nor* at high GT costs, GT may still represent a significant evolutionary force contributing to the observed *napA* distribution in extant fungal lineages (Table S3). For example, AU tests rejected the monophyly of three Ascomycota (Dothideomycetes, Leotiomycetes, and Sordariomycetes) and one Basidiomycota (Pucciniomycetes) lineage within the *napA* phylogeny (Table S2, $P \leq 0.05$). Specific instances of predicted HGT events are outlined in Supplemental Information (SI) for each gene (Table S4, Fig. S5).

Fungal P450nor evolved from actinobacterial P450s involved in SM

Previous investigations have hypothesized an actinobacterial origin for *p450nor* based on amino acid sequence alignments (7, 28, 30), but rigorous phylogenetic tests of *p450nor*'s origins were lacking to support this hypothesis. Alignment of fungal P450nor amino acid sequences to the NCBI RefSeq protein database identified 230 bacterial sequences with significant sequence alignment (≥ 65 % query coverage, ≥ 35 % amino acid identity) to P450nor. Of note, *p450nor* homologs were also detected within the genomes of three freshwater inhabiting green algae, *Chlorella variabilis*, *Chlamydomonas reinhardtii*, and *Monoraphidium neglectum*, expanding the known distribution of *p450nor* to photosynthetic eukaryotic microbes. Additional *p450nor* homologs were not detected in archaea, plant, protist, or other lineages housed within the RefSeq database. Of the bacterial cytochrome P450 (hereafter P450) sequences identified, approximately 6 % (n = 13) were proteobacterial in origin, whereas the remaining sequences belonged to members of the bacterial phylum *Actinobacteria* (Fig. S6). Ancestral character state reconstruction of select P450 families on a subset of these sequences supported the monophyly of *p450nor* and bacterial P450 gene sequences of the P450 family CYP105 (Fig. 2) (39). The same relationships were preserved when phylogenetic reconstruction was performed using the complete set of 408 P450 amino acid sequences (Fig. S7). Importantly, NO-utilizing P450 sequences from the CYP107 family belonging to members of the *Streptomyces* formed a larger monophyletic clade containing P450nor and other CYP105 sequences (Fig S7). The CYP107 family includes *txtE* genes encoding nitrating enzymes that use NO as a substrate for the production of secondary metabolites and have no known role in respiratory denitrification or detoxification (40, 41). Thus, P450nor and TxtE are related (40, 41), yet TxtE is involved in SM and is the only other P450 observed to directly utilize NO as a substrate.

Sequences of the bacterial CYP105 family of P450s include diverse actinobacterial genera such as *Streptomyces* (n = 159), *Amycolatopsis* (n = 12), *Saccharothrix* (n = 5), *Streptacidiphilus* (n = 4), *Frankia* (n = 4), *Kutzneria* (n = 4), *Nocardia* (n = 3), and members from 17 additional actinobacterial genera (n = 39). The proteobacterial sequences were affiliated with members of the genera *Burkholderia* (n = 5), *Paracoccus* (n = 3), *Bradyrhizobium* (n=3), *Pseudomonas* (n = 1), and *Halomonas* (n = 1). Bacterial P450 gene and species tree comparisons of 60% identity clustered P450 amino acid sequences (n = 57) and cognate 16S rRNA genes (n = 55) supported HGT of one or more actinobacterial P450 genes to members of the *Alpha-*, *Beta-*, and *Gammaproteobacteria* (Fig. S6). Furthermore, ancestral character state reconstruction overwhelmingly supported *Actinobacteria* as the root state (root probability = 0.99 ± 0.06) of the bacterial CYP105 family P450 phylogeny. When forcing the root state of the P450 phylogeny to be *Proteobacteria* (simple model) and comparing to the complex model where the root is allowed to vary, the simple model with a proteobacterial root was not supported (average log Bayes Factor = 0.03 ± 0.18). Therefore, *p450nor* likely evolved from one or more CYP105 family P450 genes found in members of the *Actinobacteria*. This finding underscores *p450nor*'s distinct origin compared to the fungal denitrification traits *napA* and *nirK*, which have a distinct proteobacterial ancestry consistent with the majority of bacterial denitrifiers (Fig. S8).

Widespread co-occurrence of *p450nor* and NO-detoxifying flavohemoglobins

Poor conversion of inorganic N-oxides to N_2O by fungal isolates supports the hypothesis that P450nor is involved in NO detoxification (7, 42). However, fungi also possess NO-detoxifying flavohemoglobins responsible for detoxification of NO to NO_3^- under oxic conditions or NO to N_2O under anoxic conditions (42–44). Flavohemoglobins were detected in 450 (63 %) fungal genomes investigated and were widespread within ascomycete and basidiomycete fungi. Within

p450nor-containing genomes, 125 (75 %) also possessed a flavohemoglobin gene (Fig. 1, Table S1). The number of genomes in fungal families containing *p450nor* and NO-detoxifying flavohemoglobin genes were significantly correlated (Spearman r = 0.87, $p = 1.6e^{-10}$), and suggests *p450nor*'s primary function is not NO detoxification.

Evidence of a role for *p450nor* in secondary metabolism

p450nor is actinobacterial in origin, yet *Actinobacteria* are not considered canonical denitrifiers and evidence for their role in denitrification was lacking when *p450nor* was initially identified (29, 45). Subsequent investigations did not posit a role for *p450nor* in SM despite the affiliation of *p450nor* and CYP105 P450s with documented roles in SM (34, 46). To assess genomic evidence linking *p450nor* to SM, we queried genes encoded within genomic regions approximately 50 kb on either side of *p450nor* for functions related to SM. The biosynthetic gene cluster (BGC) prediction tool antiSMASH detected putative BGCs containing *p450nor* in 19 (11 %) of the 167 *p450nor*-containing genomes analyzed (Dataset S2). The number of open reading frames in a predicted SM cluster ranged from 34 to 97, spanning 21,086 to 55,473 nucleotides in length. Inspection of protein-coding genes surrounding *p450nor* using curated antiSMASH profile Hidden Markov Models (pHHMs) resulted in the identification of hallmark SM features (e.g., polyketide synthases (PKS), non-ribosomal peptide synthases (NRPS), terpene cyclases, dimethylallyl tryptophan synthases) in an additional 40 (24 %) of the 167 *p450nor*-containing genomes analyzed (Dataset S2) (see Materials and Methods for details). The distribution of automatic and manually curated protein-coding genes surrounding a subset of 32 *p450nor*-containing fungi suggests that *p450nor*-containing BGCs are structurally and functionally diverse (Fig. 3). An additional BGC prediction tool, CASSIS, which detects BGCs based on shared transcription factor binding sites upstream and downstream of a user specified

anchor gene (47), predicted as many as 105 (63 %) *p450nor*-containing gene regions to be BGCs (Dataset S3). Furthermore, CASSIS analysis corroborated 74 % of the 19 BGCs predicted by antiSMASH (Dataset S3). A detailed accounting of antiSMASH and CASSIS predictions, gene annotations, and gene organization surrounding *p450nor* in all 167 *p450nor*-containing genomes is available in the SI (Fig. S9, Dataset S2).

A diversity of secondary metabolite biosynthesis pathways were predicted to be encoded by *p450nor*-containing BGCs, including nonribosomal peptides (n = 7), polyketides (n = 5), terpenes (n = 2), hybrid terpene-polyketide-indoles (n = 2), indoles (n = 1), or currently unclassifiable compounds (n = 2). Phylogenetic reconstruction of C-type and ketosynthase domains encoded by NRPS and PKS genes surrounding *p450nor* enabled the prediction of potential secondary metabolites encoded by fungal *p450nor*-containing BGCs (Fig. 4). For example, domains from NRPS and PKS sequences encoded nearby *p450nor* are affiliated with reference NRPS and PKS sequences known to produce cyclic tetrapeptides (HC-toxins) (n=7), aflatoxins (n=5), fumonisins (n=4), calcium-dependent antibiotics (n=1), and statins (n=1), suggesting a large variety of secondary metabolites are encoded by gene regions containing *p450nor*.

The formation of N_2O has previously been reported as highly variable among closely related fungi (37, 48), yet evidence suggesting a role for *p450nor* in this phenomenon is lacking. Of the 94 fungal genera harboring *p450nor*, 21 (22 %) contained species with and without a copy of *p450nor* (Table S5). For example, 15 out of 16 (94 %) *Pseudogymnoascus* genomes contained *p450nor*, whereas only 1 out of 7 (14 %) *Exophiala* genomes contained a *p450nor* gene. Nucleotide alignments of *p450nor*-containing genomic regions (81.3 ± 27.8 kb in length) against other fungal genomes revealed a disproportionately high nucleotide identity and alignment

length between genomes with and without *p450nor* from the same genus (Fig. 5A-C). For example, genomic regions surrounding *p450nor* in *Exophiala xenobiotica* are highly similar to other *Exophiala* species without *p450nor* (Fig. 5D), and additional examples of large, high identity regions between closely related fungal genomes with and without *p450nor* are abundant (Fig. 5A-C, Dataset S4).

Discussion

An evaluation of hypotheses regarding the biological role of *p450nor*

The three leading hypotheses regarding the biological role of fungal *p450nor* are respiratory denitrification (7), NO detoxification (42), and now secondary metabolism. The respiratory denitrification hypothesis is dubious since evidence is lacking to classify fungi as respiratory denitrifiers (4, 17–19, 49). Furthermore, unaccounted for methodological biases inherent to partitioning techniques raises substantial concerns over the validity of fungal N_2O production *in situ* (4, 25–27). The ineffectiveness of antibiotics to partition microbial respiration has been previously demonstrated (25, 26), yet antibiotics continue to be used to support the prevalence of fungal respiratory denitrification. In addition to antibiotic inhibition, site preference measurements of the intramolecular distribution of ^{15}N within the linear N_2O molecule (i.e., N_2O isotopocules) of cultured microorganisms have been increasingly applied to partition microbial sources of N_2O *in situ* (5, 50). Although promising, the limitations of N_2O isotopocule measurements used in isolation are becoming apparent (27, 51, 52). Of primary concern is the significant overlap in, and difficulty discretizing, site preference measurements of distinct processes or diverse microbial assemblages (51, 53, 54). Therefore, the respiratory denitrification

hypothesis is predicated on biased approaches used in isolation that are unable to correctly assess fungal contributions to denitrification.

Another alternative function suggested for P450nor is NO detoxification, which was initially postulated in experiments using the fungus *Fusarium oxysporum* strain 11n1 (55). This hypothesis was supported by low growth yields and a poor mass balance between the N-oxyanion inputs and N_2O formed (18, 56, 57). Although plausible, the NO detoxification hypothesis is confounded by extensive co-occurrence between *p450nor* and genes encoding canonical NO-detoxifying flavohemoglobins, which also produce N_2O (44, 58) (Fig. 1, Table S1). Considering the extensive overlap in *p450nor* and flavohemoglobin gene presence (Fig.1), the utility of site preference values derived from N_2O formed by fungi in pure culture is questionable. Furthermore, P450nor and flavohemoglobins would likely compete for NO under anoxic conditions, and experiments teasing apart their contributions to N_2O formation are necessary to support the postulated role of P450nor in NO detoxification. The reported Michaelis constant (K_m) of NO binding to P450nor ranges from 0.1 to 0.6 mM (11, 12) and is orders of magnitude higher than the 0.1 to 0.25 μM K_m reported for flavohemoglobins (59), suggesting flavohemoglobin would outcompete P450nor for NO binding. Hence, the higher affinity of flavohemoglobins for NO and their greater distribution in fungi would suggest a limited role for P450nor in NO detoxification (Table S1). Though fungi certainly detoxify NO, insufficient evidence exists to attribute this activity to P450nor.

The SM hypothesis has traction considering that P450nor is derived from CYP105 P450s (Fig. 2), all of which share a functional role in SM (34, 46, 60). Thus, the adaptation of P450nor to a novel niche in NO reduction and denitrification is unlikely. A more parsimonious hypothesis is that P450nor has maintained a role in SM as observed for related actinobacterial enzymes.

When *p450nor* was originally described, members of the *Actinobacteria* (e.g., *Streptomyces*) were already well established secondary metabolite producers and their N_2O production was attributed to detoxification (45, 61). The monophyly of P450nor with the SM enzyme TxtE, the only other NO-utilizing P450, provides additional *a priori* support for P450nor's role in SM (Fig. S7). P450nor's role in SM is further corroborated by SM prediction tools where a sizeable proportion (35 %) of gene regions surrounding *p450nor* contained genes predicted to encode hallmark SM functions, and as many as 105 (63 %) *p450nor*-containing genomic regions were automatically predicted to be involved in SM (Fig. 3). Moreover, the fact that antiSMASH flagged 11% of *p450nor*-containing genomic regions as putative BGCs suggests their organization and gene content is highly similar to other characterized BGCs. Although phylogenomic evidence supports a role for P450nor in the biosynthesis of secondary metabolites, direct physiological evidence should be a target for future research efforts. Emerging technologies enabling the expression of full length BGCs and metabolite identification should enable robust experimentation to test the SM hypothesis (62). Regardless, *p450nor*-containing genomic regions were predicted to be BGCs encoding diverse metabolites including terpenoids, nonribosomal peptides, polyketides, indoles, and other complex metabolites (Fig. 4) consistent with its evolutionary origins (Fig. 2).

Predicting P450nor's role in secondary metabolism

A variety of metabolites containing nitro functional groups have been detected in fungal genera known to harbor denitrifying representatives (63), yet mechanistic explanations for nitration reactions in fungi remain elusive. The addition of a nitro functional group to a metabolite represents a potential mechanism for enhancing its toxicity or functional specificity (64). The hypothesis of a role for P450nor in nitration, or possibly nitrosylation, of fungal metabolites is

355 attractive given P450nor's affiliation with the nitrating enzyme TxtE. The inclusion of *p450nor*
356 within BGCs may be adaptive in fungal lineages in which this gene was acquired due to the
357 augmenting effects that nitro or nitroso groups impart on their substrates (64). Support for this
358 hypothesis stems from the widespread distribution of *p450nor* within secondary metabolite
359 producing members of the Ascomycota (65, 66), and previous reports of HGT between members
360 of *Actinobacteria* and fungi in enhancing fungal SM (67). Furthermore, the high nucleotide
361 identity shared between *p450nor*-containing genomic regions from closely related fungal species
362 suggests *p450nor* gain or loss may have important consequences for the secondary metabolites
363 potentially produced by *p450nor*-containing BGCs (Fig. 5D). Considering that 22 *p450nor*
364 containing fungal genera display variability in *p450nor* presence/absence (Table S5),
365 investigations regarding the impact of *p450nor* presence/absence on the secondary metabolite
366 pool, fungal fitness, competition, or infectivity within closely related fungi is readily testable.
367 Additional unknowns related to P450nor's role in SM are the identification of putative
368 substrates and sources of NO required to fuel the hypothesized nitration or nitrosylation
369 reactions. To date, P450nor is solely reported to bind the electron donors NADH or NADPH and
370 the electron acceptor NO (7). However, N_2O formation by P450nor is oxygen dependent (8, 22),
371 suggesting O_2 may be an additional substrate as observed for TxtE (40). TxtE and NovI, both
372 P450s affiliated with P450nor, bind to and transform L-tryptophan and L-tyrosine to produce the
373 secondary metabolites thaxtomin A and novobiocin, respectively (40, 68). It is conceivable that
374 P450nor might also bind O_2 and aromatic amino acids, but direct experimental evidence is
375 required to support this hypothesis. A potential source of NO in fungi could result from nitrite
376 reductase activity of the copper containing nitrite reductase, NirK. The NO synthase (TxtD) from
377 *Streptomyces turgidiscabies* produces NO to fuel TxtE nitration of L-tryptophan (40), but *txtD*

homologs were not detected in the fungal genomes examined. Although evidence of NO synthases in fungi exist, knowledge regarding their distribution is limited (69, 70). Given the functional redundancy between NO synthases and NirK, it is conceivable that one of NirK's functions in fungi is to generate NO for use by P450nor in SM.

Causes and consequences of *p450nor* evolution in fungi

A limited understanding of *p450nor* evolution represented an impediment to our knowledge of fungal N_2O formation. For example, closely related fungi vary in their ability to produce N_2O (16, 37, 48, 56), and the evolutionary forces (e.g., HGT, gene gain/loss, and incomplete lineage sorting) contributing to this observation were unexplored. For *p450nor*, many HGT events were observed between distantly related fungal lineages using gene and species tree comparisons (Fig. S2). Although HGT events are challenging to precisely quantify given the level of uncertainty in deeply branching nodes of the functional gene trees reported here, a signal of potentially double digit HGT events were observed using gene tree-species tree reconciliation (Table S3). Moreover, genetic elements encoding *pogo* family transposases (N = 9), retrotransposons (N = 4), and reverse transcriptases (N = 1) were in some cases detected adjacent to *p450nor* and may act as vehicles for dissemination of *p450nor* within fungi and between fungal chromosomes (Dataset S2).

N_2O production was previously coined a widespread trait in fungi (37), yet genomic analysis suggests fortuitous N_2O formation by fungi is largely restricted to members of the Ascomycota. For example, of the167 *p450nor*-containing fungal genomes identified, 163 were affiliated with members of the Ascomycota and only four with members of the Basidiomycota. N_2O production has been reported for fungal isolates assigned to the recently revised phylum Mucoromycota (4, 71), yet no evidence of genes underlying denitrification were detected in

available genomes from members of this phylum (Fig. 1). Denitrification markers were also absent from ascomycete yeast genomes (i.e., *Candida*, *Yarrowia*), though a number of N_2O-producing ascomycete yeasts have been reported (56). Even within the Basidiomycota, N_2O formation is restricted to a few taxa within the Tremellomycetes and Agaricomycetes (4), and at least for members of the Tremellomycetes, was likely the result of HGT from one or more members of the Ascomycota (Fig S2). The finding that genomes from fungi (e.g., ascomycete yeasts) previously observed to produce N_2O did not possess denitrification traits was unexpected and suggests that experimental artifacts or other mechanisms, such as the NO-detoxifying activity of flavohemoglobins, may also contribute to N_2O formation in fungi. In addition to fungi, species of green algae have been reported to produce small quantities of N_2O, the production of which could, at least in part, be attributed to the presence of *p450nor* within this lineage (72–74). Despite these findings, green algae lack a mass balance between the inorganic N added and the N_2O formed (74) and display low rates and quantities of N_2O production on par with fungi (72), suggesting that N_2O formation is not a respiratory process in these organisms. Considering the lack of evidence of respiratory denitrification in green algae and genomic evidence linking *p450nor* to SM in fungi, the SM hypothesis is an attractive explanation for the presence of *p450nor* in green algae as well.

p450nor genes within fungi also have implications for fungal pathogenesis (4). At least for some bacteria (e.g., *Neisseria*, *Brucella*, *Mycobacterium*), the presence of denitrification genes has been demonstrated to enhance virulence or detoxification of N-oxides produced by the host (75). Although the impact of denitrification gene acquisition on fungal pathogenesis is not well established, there is growing evidence for P450nor involvement in fungal virulence (4, 7). For example, *p450nor* gene expression is linked to *Fusarium* wilt in banana and cotton plants,

yet mechanistic explanations of P450nor's function during plant infection are lacking (76, 77). Notably, more than half of all *p450nor*-containing fungal species are known plant pathogens (4), and the involvement of *p450nor* in SM is consistent with and would support the plant pathogenic life history strategies of many *p450nor*-containing fungi.

The diversity of denitrifying microorganisms and the modularity of the pathway has led to the view of denitrification as a community function (78–80). Therefore, limited co-occurrence and correlated evolution between *napA, nirK*, and *p450nor* might suggest mutualistic interactions occur between fungal or bacterial species performing denitrification. However, gene co-occurrences and evolutionary correlations should be interpreted with caution as additional factors (e.g., shared ecological niche, selection pressures) related to fungal life history strategies may explain their distribution equally well. For example, N_2O-producing fungi are frequently detected in, and cultivated from, highly disturbed, N-amended agricultural soils (4, 9, 16) and detoxification or N-oxide utilization traits may merely co-occur more frequently due to selection imposed by episodic N addition. Fungi also contain genes homologous to bacterial denitrifiers, but their presence does not guarantee a role in respiratory denitrification. For example, the presence of genes homologous to the bacterial NO reductase (*norB*) is not sufficient evidence for respiratory denitrification potential in bacteria (17, 75). The same is true of the abundant *napA* gene homologs detected in fungal genomes, which would suggest a robust capacity of fungi to perform dissimilatory nitrate reduction. Yet this is not the case, and many fungi only produce N_2O when NO_2^- is present (4, 18, 56).

In summary, fungi often produce little or no gaseous N from reduction of N-oxyanions and do not grow proportionally to the quantity of N-oxyanions consumed; thus, fungi cannot be classified as respiratory denitrifiers (17). Given the limited accounting of methodological bias in

the study of N_2O production by fungi (25–27), alternative explanations for the biological function of *p450nor* in fungi are likely and raises concerns over the validity of these techniques in estimating fungal contributions to N_2O emissions. Although the P450nor NO detoxification hypothesis is plausible, available data are insufficient at present to definitively support a role for P450nor in this process. Considering that many canonical denitrifying fungi are also plant disease causing secondary metabolite producers and agricultural pests, the affiliation of *p450nor* with non-denitrifying actinobacterial sequences involved in SM and their inclusion in BGCs strongly endorses a biological role for *p450nor* in SM.

Materials and Methods

Datasets

Draft and complete fungal, algal, and bacterial genomes were accessed from the National Center for Biotechnology Information and the Joint Genome Institute on March 16th, 2016 and downloaded from their respective database utilities. A list of fungal, algal, and bacterial genomes and their taxonomic and database affiliations can be found in the Supplemental Information (SI) (Dataset S5).

Gene marker identification

To identify gene markers within fungal genomes suitable for phylogenetic analysis, a database of 1,438 amino acid sequences of fungal single copy orthologs from the BUSCO tool v1.1b (81) were provided as queries to the genblastG search tool v1.0.138 (82). The genblastG tool performs amino acid alignment of protein queries against a six frame translated nucleotide subject sequence (genome) to find significant alignments and uses heuristic analysis to piece the appropriate gene models back together from high-scoring segment pairs identified using BLAST (83). Of the BUSCO gene models queried, 238 were used for phylogenetic tree reconstruction

and were annotated using PfamScan against the Pfam A database and blastp against the uniprot database with default settings (84–87) (Dataset S6). The genblastG tool was also used to detect gene sequences involved in denitrification (NapA, NarG, NirK/NirS, NorB, P450nor, NosZ) from curated bacterial proteins in the FunGene repository (88) or proteins involved in NO detoxification (flavohemoglobins) identified in the literature (44). Denitrification gene models used in downstream phylogenetic analysis were manually curated against full length fungal reference sequences to ensure that accurate gene models were predicted for each organism in which the gene was detected. After identification of these genes in fungal genomes, alignment of the fungal NapA, NirK, NarG, and P450nor amino acid sequences with blastp against the plant, archaea, bacteria, protozoa, and fungi RefSeq protein databases (89) was performed to identify similar sequences in each taxonomic group. Protein sequences demonstrating significant alignment (≥ 60 % query coverage and ≥ 35 % amino acid identity) to fungal proteins were used in subsequent phylogenetic reconstructions.

Gene prediction for comparative genomic analyses

The *ab initio* gene predictor SNAP (90) was used to predict gene models in fungal genomes where no such information was available (e.g., some draft genomes). In this case, one or several closely related fungal genomes containing gene models were selected based on phylogenetic affiliation to train SNAP for gene prediction. Although this methodology is limiting when closely related genomes are unavailable, gene models from close relatives were available for *p450nor*-containing genomes lacking gene predictions.

Alien index calculations

The alien index (AI) was calculated as previously described and modified for use with a single gene (44). Briefly, pairwise amino acid sequence alignments were performed using blastp for

fungal NapA, NirK, and P450nor sequences. The in group was defined as the aligned sequence with the highest bitscore (excluding the query) belonging to the same taxonomic class as the query sequence. Accordingly, the out group was defined as the aligned sequence with the highest bitscore not belonging to the same taxonomic class as the query. The maximum bitscore was the bitscore derived from the alignment of the query to itself. Therefore, AI is calculated as follows:

$$AI = (out\ group\ bitscore / \max bitscore) - (in\ group\ bitscore / \max bitscore)$$

AI values range from 1 to -1. Values greater than zero are indicative of HGT or contamination of foreign DNA within the genome sequence being queried.

Analysis of SM gene clusters in fungi

Genomic regions 50 kb up- and downstream of a *p450nor* gene in each genome were subjected to gene cluster prediction with the antiSMASH and CASSIS tools with default settings (47, 91). Additionally, genes encoded +/- 10 genes up and downstream of *p450nor* were evaluated using PfamScan searches with default settings against the pHHMs of curated SM genes identified by antiSMASH (Dataset S2) (91). Protein sequences with significant alignment to antiSMASH pHMMs were given an "automatic" SM function status and were colored blue. In order to supplement the automated SM annotation, additional functional annotation was performed by hmmscan searches with HMMER3 (92) against the eggNOG database (93). These functional annotations were manually flagged as related to SM if they possessed literature entries suggesting an involvement in SM or had functions related to methyl transfer, oxidation-reduction reactions, glycosyl transferases, fungal specific transcription factors, and other protein functions that may be important for SM outlined by antiSMASH (91). All manual SM annotations were colored light blue to indicate potential involvement in SM. All other annotations were colored grey when no evidence connecting the function to SM could be identified.

Additionally, ortholog clustering of protein-coding genes surrounding *p450nor* was performed using OrthoFinder (94) with default settings. Ortholog clustering was performed using only a representative *p450nor* loci in each fungal genome if multiple gene copies were present. A Shannon-like diversity index of fungal classes detected in each orthologous group was calculated as $H' = -\sum(P_i * \ln(P_i))$, where P_i is the fraction of fungal class *i* present in an orthologous group. Pairwise nucleotide alignments of *p450nor*-containing genomic regions were performed as previously described (95). Briefly, the *nucmer* utility of MUMmer *v3.0* (96) was used to align *p450nor*-containing genomic regions (~100 kb) against whole genomes of fungi with and without *p450nor*. The average nucleotide identity (reported as ANIm) of the alignment was calculated from the resulting delta output file. The resulting data was plotted using Matplotlib (97) available for the python programming language (http://www.python.org).

Phylogenetic analysis

Phylogenetic reconstruction of the fungal species tree was performed using concatenated amino acid sequences from 238 single copy orthologs found in ≥ 90 % of all genomes (Dataset S6). The genomes of *Puccinia arachidis* and *Microbotryum lychnidis-dioicae* strain p1A1 Lamole were excluded from further analysis due to an insufficient number of informative sites and inconsistent placement within the fungal tree. Alignment of amino acid sequences were performed individually on all 238 individual BUSCO gene models present within each organism using MAFFT v7.130b (98) with linsi alignment tuning parameters (--maxiterate 1000 and --localpair settings used). Individual alignments were concatenated using in-house python scripts, resulting in a 65,897 column alignment. Tree reconstruction was performed using FastTree2 (99) with refined tree reconstruction settings for slower, more exhaustive search of the tree space than default settings (-bionj -slow -gamma -spr 4 -lg -mlacc 2 and -slownni settings). For comparison

to tree reconstruction using a concatenated alignment, individual trees from each BUSCO alignment were also constructed using FastTree2 with identical settings as above. The resultant alignments and trees were subjected to coalescent tree reconstruction using ASTRAL-II software (100). Overall, both phylogenies largely agreed except for branching patterns of some lineages (e.g., Zoopagomycota and Mucoromycota) and are available online in a figshare repository (see *Data Sharing* below)

The predicted amino acid and intronless nucleotide sequences of fungal *napA*, *nirK*, and *p450nor* gene models were aligned using the MAFFT settings described above and manually refined in JalView and SeaView software (101, 102). Maximum-likelihood (ML) and Bayesian phylogenetic tree reconstruction was performed on both nucleotide and amino acid alignments using RAxML and MrBayes, respectively (103, 104). Selection of the optimal evolutionary model for ML tree reconstruction was performed using prottest (105) (amino acid alignment) and jmodeltest (106) (nucleotide alignment) software prior to ML tree reconstruction. Please refer to SI for additional details about evolutionary models used in phylogenetic analysis.

Phylogenetic analysis with RAxML was performed by sampling 20 starting trees and performing 1,000 replicate bootstrap analyses. The tree with the maximal negative log likelihood score was compared to 1,000 replicates in RAxML to generate the final tree. Bayesian tree construction was performed using 3 independent runs with 6 chains for 5,000,000 generations. Output from MrBayes was evaluated with the sump and sumt commands within the software to ensure Markov Chain Monte Carlo chain mixing and convergence (potential scale reduction factor of 1.0) and standard deviation of split frequencies ~ 0.01 or lower. MrBayes output was further visualized in the program Tracer (http://tree.bio.ed.ac.uk/software/tracer/) to ensure convergence was reached.

BayesTraits software was used to perform phylogenetically informed correlations between binary traits (i.e., the presence or absence of two denitrification markers) and ancestral state reconstruction (107). Please refer to SI for additional details on BayesTraits analyses.

Approximately unbiased (AU) tests were performed in the program CONSEL (108) using default settings. The negative log likelihood values from the observed nucleotide phylogenies input into CONSEL were -140,261, -37,782, -111,531 for *napA*, *nirK* and *p450nor*, respectively. The observed negative log likelihood scores for amino acid phylogenies of NapA, NirK, and P450nor were -65,158, -14,197, and -44,171, respectively. Species-tree gene-tree reconciliation was performed using NOTUNG software v2.9 (38, 109). Please see SI for further details on NOTUNG parameters.

Statistical analysis

All statistical analyses were carried out in R programming language (110) and significance of statistical tests were assessed using a p value cutoff ≤ 0.05.

Data sharing

All gene models, alignments, and trees discussed in the manuscript are made available in a figshare repository prepared by S.A.H. (https://doi.org/10.6084/m9.figshare.c.3845692).

Acknowledgements

We thank Gerald Bills, Gregory Bonito, Pedro Crous, Kathryn Bushley, Colleen Hansel, Patrik Inderbitzin, Gabor Kovacs, Bjorn Lindahl, Jon Magnuson, Francis Martin, Kerry O'Donnell, Nancy Nichols, Minou Nowrousian, and Joseph Spatafora for providing access to unpublished genome data produced by the U.S. Department of Energy Joint Genome Institute. The authors thank A. Frank for assistance with manuscript revisions. S.A.H. would like to acknowledge a Department of Energy Office of Science Graduate Student Research fellowship for support

during preparation of the manuscript. Participation of C.W.S and F.E.L. was partially sponsored by the Laboratory Directed Research and Development Program of Oak Ridge National Laboratory, managed by UT-Battelle, LLC, for the U. S. Department of Energy. This research was partially supported by the US Department of Energy, Office of Biological and Environmental Research, Genomic Science Program, Award DE-SC0006662.

References

1. **Canfield DE**, **Glazer AN**, **Falkowski PG**. 2010. The evolution and future of Earth's nitrogen cycle. Science **330**:192–6.

2. **Galloway JN**, **Townsend AR**, **Erisman JW**, **Bekunda M**, **Cai Z**, **Freney JR**, **Martinelli L a**, **Seitzinger SP**, **Sutton M a**. 2008. Transformation of the nitrogen cycle: Recent trends, questions, and potential solutions. Science (80-.). **320**:889–892.

3. **Zumft WG**. 1997. Cell biology and molecular basis of denitrification. Microbiol. Mol. Biol. Rev. **61**:533–616.

4. **Mothapo N**, **Chen H**, **Cubeta MA**, **Grossman JM**, **Fuller F**, **Shi W**. 2015. Phylogenetic, taxonomic and functional diversity of fungal denitrifiers and associated N_2O production efficacy. Soil Biol. Biochem. **83**:160–175.

5. **Wankel SD**, **Ziebis W**, **Buchwald C**, **Charoenpong C**, **de Beer D**, **Dentinger J**, **Xu Z**, **Zengler K**. 2017. Evidence for fungal and chemodenitrification based N_2O flux from nitrogen impacted coastal sediments **8**:15595.

6. **Cathrine SJ**, **Raghukumar C**. 2009. Anaerobic denitrification in fungi from the coastal marine sediments off Goa, India. Mycol. Res. **113**:100–109.

7. **Shoun H**, **Fushinobu S**, **Jiang L**, **Kim S-W**, **Wakagi T**. 2012. Fungal denitrification and nitric oxide reductase cytochrome P450nor. Philos. Trans. R. Soc. Lond. B. Biol. Sci. **367**:1186–94.

8. **Mothapo N V**, **Chen H**, **Cubeta MA**, **Shi W**. 2013. Nitrous oxide producing activity of diverse fungi from distinct agroecosystems. Soil Biol. Biochem. **66**:94–101.

9. **Chen H**, **Mothapo N V**, **Shi W**. 2014. The significant contribution of fungi to soil N_2O production across diverse ecosystems. Appl. Soil Ecol. **73**:70–77.

10. **Hu H-W**, **Chen D**, **He J-Z**. 2015. Microbial regulation of terrestrial nitrous oxide formation: understanding the biological pathways for prediction of emission rates. FEMS Microbiol. Rev. **39**:729–749.

11. **Shiro Y**, **Fujii M**, **Iizuka T**, **Adachi S**, **Tsukamoto K**, **Nakahara K**, **Shoun H**. 1995. Spectroscopic and kinetic studies on reaction of cytochrome P450nor with nitric oxide: Implication for its nitric oxide reduction mechanism. J. Biol. Chem. **270**:1617–1623.

12. **Nakahara K**, **Tanimoto T**, **Hatano K**, **Usuda K**, **Shoun H**. 1993. Cytochrome P-450 55A1 (P-450dNIR) acts as nitric oxide reductase employing NADH as the direct electron donor. J. Biol. Chem. **268** :8350–8355.

13. **Shimizu H**, **Park S-Y**, **Shiro Y**, **Adachi S**. 2002. X-ray structure of nitric oxide reductase (cytochrome P450nor) at atomic resolution. Acta Crystallogr. Sect. D **58**:81–89.

14. **Novinscak A**, **Goyer C**, **Zebarth BJ**, **Burton DL**, **Chantigny MH**, **Filion M**. 2016. Novel *P450nor* gene detection assay used to characterize the prevalence and diversity of soil fungal denitrifiers. Appl. Environ. Microbiol. **82**:4560–4569.

15. **Li Y**, **Liu Q**, **Liang X**, **Xiao Q**, **Fang Y**, **Wu Y**. 2016. A new fluorescence biosensor for nitric oxide detection based on cytochrome P450 55B1. Sensors Actuators B Chem. **230**:405–410.

16. **Higgins SA**, **Welsh A**, **Orellana LH**, **Konstantinidis KT**, **Chee-Sanford JC**, **Sanford RA**, **Schadt CW**, **Löffler FE**. 2016. Detection and diversity of fungal nitric oxide reductase genes (*p450nor*) in agricultural soils. Appl. Environ. Microbiol. **82**:2919–2928.

17. **Mahne I**, **Tiedje JM**. 1995. Criteria and methodology for identifying respiratory denitrifiers. Appl. Environ. Microbiol. **61**:1110–1115.

18. **Shoun H**. 1992. Denitrification by fungi. FEMS Microbiol. Lett. **94**:277–281.

19. **Tsuruta S**, **Takaya N**, **Zhang L**, **Shoun H**, **Kimura K**, **Hamamoto M**, **Nakase T**. 1998. Denitrification by yeasts and occurrence of cytochrome P450nor in *Trichosporon cutaneum*. FEMS Microbiol. Lett. **168**:105–110.

20. **Bleakley BH**, **Tiedje JM**. 1982. Nitrous oxide production by organisms other than nitrifiers or denitrifiers. Appl. Environ. Microbiol. **44** :1342–1348.

21. **Stief P**, **Fuchs-Ocklenburg S**, **Kamp A**, **Manohar C-S**, **Houbraken J**, **Boekhout T**, **de Beer D**, **Stoeck T**. 2014. Dissimilatory nitrate reduction by *Aspergillus terreus* isolated from the seasonal oxygen minimum zone in the Arabian Sea. BMC Microbiol. **14**:35.

22. **Zhou Z**, **Takaya N**, **Sakairi MAC**, **Shoun H**. 2001. Oxygen requirement for denitrification by the fungus *Fusarium oxysporum*. Arch. Microbiol. **175**:19–25.

23. **Shoun H**, **Tanimoto T**. 1991. Denitrification by the fungus *Fusarium oxysporum* and involvement of cytochrome P-450 in the respiratory nitrite reduction. J. Biol. Chem. **266**:11078–11082.

24. **Herold MB**, **Baggs EM**, **Daniell TJ**. 2012. Fungal and bacterial denitrification are differently affected by long-term pH amendment and cultivation of arable soil. Soil Biol. Biochem. **54**:25–35.

25. **Rousk J**, **Demoling LA**, **Bååth E**. 2009. Contrasting short-term antibiotic effects on respiration and bacterial growth compromises the validity of the selective respiratory inhibition technique to distinguish fungi and bacteria. Microb. Ecol. **58**:75–85.

26. **Ladan S**, **Jacinthe P-A**. 2016. Evaluation of antibacterial and antifungal compounds for selective inhibition of denitrification in soils. Environ. Sci. Process. Impacts.

27. **Phillips RL**, **Song B**, **McMillan AMS**, **Grelet G**, **Weir BS**, **Palmada T**, **Tobias C**. 2016. Chemical formation of hybrid di-nitrogen calls fungal codenitrification into question. Sci. Rep. **6**:39077.

28. **Moktali V**, **Park J**, **Fedorova-Abrams N**, **Park B**, **Choi J**, **Lee Y-H**, **Kang S**. 2012. Systematic and searchable classification of cytochrome P450 proteins encoded by fungal and oomycete genomes. BMC Genomics **13**:525.

29. **Kizawa H**, **Tomura D**, **Oda M**, **Fukamizu A**, **Hoshino T**, **Gotoh O**, **Yasui T**, **Shoun H**. 1991. Nucleotide sequence of the unique nitrate/nitrite-inducible cytochrome P-450 cDNA from *Fusarium oxysporum*. J. Biol. Chem. **266**:10632–10637.

30. **Chen W**, **Lee M-K**, **Jefcoate C**, **Kim S-C**, **Chen F**, **Yu J-H**. 2014. Fungal cytochrome

P450 monooxygenases: their distribution, structure, functions, family expansion, and evolutionary origin. Genome Biol. Evol. **6**:1620–1634.

31. **Shoun H**, **Kano M**, **Baba I**, **Takaya N**, **Matsuo M**. 1998. Denitrification by actinomycetes and purification of dissimilatory nitrite reductase and azurin from *Streptomyces thioluteus*. J. Bacteriol. **180**:4413–4415.

32. **Shapleigh JP**. 2013. Denitrifying prokaryotes, p. 405–425. *In* Rosenberg, E, DeLong, EF, Lory, S, Stackebrandt, E, Thompson, F (eds.), The prokaryotes: Prokaryotic physiology and biochemistry. Springer Berlin Heidelberg, Berlin, Heidelberg.

33. **Kumon Y**, **Sasaki Y**, **Kato I**, **Takaya N**, **Shoun H**, **Beppu T**. 2002. Codenitrification and denitrification are dual metabolic pathways through which dinitrogen evolves from nitrate in *Streptomyces antibioticus*. J. Bacteriol. **184**:2963–2968.

34. **Moody SC**, **Loveridge EJ**. 2014. CYP105—diverse structures, functions and roles in an intriguing family of enzymes in *Streptomyces*. J. Appl. Microbiol. **117**:1549–1563.

35. **Blackwell M**, **Hibbett DS**, **Taylor JW**, **Spatafora JW**. 2006. Research coordination networks: a phylogeny for kingdom Fungi (Deep Hypha). Mycologia **98**:829–837.

36. **Martin F**, **Cullen D**, **Hibbett D**, **Pisabarro A**, **Spatafora JW**, **Baker SE**, **Grigoriev I V**. 2011. Sequencing the fungal tree of life. New Phytol. **190**:818–821.

37. **Maeda K**, **Spor A**, **Edel-Hermann V**, **Heraud C**, **Breuil M-C**, **Bizouard F**, **Toyoda S**, **Yoshida N**, **Steinberg C**, **Philippot L**. 2015. N_2O production, a widespread trait in fungi. Sci. Rep. **5**.

38. **Stolzer M**, **Lai H**, **Xu M**, **Sathaye D**, **Vernot B**, **Durand D**. 2012. Inferring duplications, losses, transfers and incomplete lineage sorting with nonbinary species trees. Bioinforma. **28** :i409–i415.

39. **Nelson DR**. 2009. The cytochrome P450 homepage. Hum. Genomics **4**:59–65.

40. **Barry SM**, **Kers JA**, **Johnson EG**, **Song L**, **Aston PR**, **Patel B**, **Krasnoff SB**, **Crane BR**, **Gibson DM**, **Loria R**, **Challis GL**. 2012. Cytochrome P450–catalyzed L-tryptophan nitration in thaxtomin phytotoxin biosynthesis. Nat Chem Biol **8**:814–816.

41. **Dodani SC**, **Cahn JKB**, **Heinisch T**, **Brinkmann-Chen S**, **McIntosh JA**, **Arnold FH**.

2014. Structural, functional, and spectroscopic characterization of the substrate scope of the novel nitrating cytochrome P450 TxtE. Chembiochem **15**:2259–2267.

42. **Morozkina E V.**, **Kurakov A V.** 2007. Dissimilatory nitrate reduction in fungi under conditions of hypoxia and anoxia: A review. Appl. Biochem. Microbiol. **43**:544–549.

43. **Poole RK**, **Hughes MN**. 2000. New functions for the ancient globin family: bacterial responses to nitric oxide and nitrosative stress. Mol. Microbiol. **36**:775–783.

44. **Wisecaver JH**, **Alexander WG**, **King SB**, **Todd Hittinger C**, **Rokas A**. 2016. Dynamic evolution of nitric oxide detoxifying flavohemoglobins, a family of single-protein metabolic modules in *Bacteria* and Eukaryotes. Mol. Biol. Evol.

45. **Kaspar HF**. 1982. Nitrite reduction to nitrous oxide by propionibacteria: Detoxification mechanism. Arch. Microbiol. **133**:126–130.

46. **O'Keefe DP**, **Harder PA**. 1991. Occurrence and biological function of cytochrome P450 monooxygenases in the actinomycetes. Mol. Microbiol. **5**:2099–2105.

47. **Wolf T**, **Shelest V**, **Nath N**, **Shelest E**. 2016. CASSIS and SMIPS: promoter-based prediction of secondary metabolite gene clusters in eukaryotic genomes. Bioinforma. **32**:1138–1143.

48. **Shoun H**. 1992. Fungal denitrification and cytochrome P-450. J. Agric. Chem. Soc. Japan **66**:154–157.

49. **Guengerich FP**, **Munro AW**. 2013. Unusual cytochrome P450 enzymes and reactions. J. Biol. Chem. **288**:17065–17073.

50. **Toyoda S**, **Yoshida N**, **Koba K**. 2017. Isotopocule analysis of biologically produced nitrous oxide in various environments. Mass Spectrom. Rev. **36**:135–160.

51. **Yang H**, **Gandhi H**, **Ostrom NE**, **Hegg EL**. 2014. Isotopic fractionation by a fungal P450 nitric oxide reductase during the production of N_2O. Environ. Sci. Technol. **48**:10707–10715.

52. **Decock C**, **Six J**. 2013. How reliable is the intramolecular distribution of ^{15}N in N_2O to source partition N_2O emitted from soil? Soil Biol. Biochem. **65**:114–127.

53. **Baggs EM**. 2008. A review of stable isotope techniques for N_2O source partitioning in soils: recent progress, remaining challenges and future considerations. Rapid Commun. Mass Spectrom. **22**:1664–1672.

54. **Butterbach-Bahl K**, **Baggs EM**, **Dannenmann M**, **Kiese R**, **Zechmeister-Boltenstern S**. 2013. Nitrous oxide emissions from soils: how well do we understand the processes and their controls? Philos. Trans. Biol. Sci. **368**:1–13.

55. **Kurakov A V**, **Nosikov AN**, **Skrynnikova E V**, **L'vov NP**. 2000. Nitrate reductase and nitrous oxide production by *Fusarium oxysporum* 11dn1 under aerobic and anaerobic conditions. Curr. Microbiol. **41**:114–119.

56. **Tsuruta S**, **Takaya N**, **Zhang L**, **Shoun H**, **Kimura K**, **Hamamoto M**, **Nakase T**. 1998. Denitrification by yeasts and occurrence of cytochrome P450nor in *Trichosporon cutaneum*. FEMS Microbiol. Lett. **168**:105–110.

57. **Rohe L**, **Anderson T**, **Braker G**, **Flessa H**, **Giesemann A**, **Lewicka-Szczebak D**, **Wrage-Monnig N**, **Well R**. 2014. Dual isotope and isotopomer signatures of nitrous oxide from fungal denitrification - a pure culture study. Rapid Commun. Mass Spectrom. **28**:1893–1903.

58. **Zumft WG**. 2005. Nitric oxide reductases of prokaryotes with emphasis on the respiratory, heme–copper oxidase type. J. Inorg. Biochem. **99**:194–215.

59. **Gardner PR**, **Gardner AM**, **Martin LA**, **Dou Y**, **Li T**, **Olson JS**, **Zhu H**, **Riggs AF**. 2000. Nitric-oxide dioxygenase activity and function of flavohemoglobins: Sensitivity to nitric oxide and carbon monoxide inhibition. J. Biol. Chem. **275**:31581–31587.

60. **Yasutake Y**, **Imoto N**, **Fujii Y**, **Fujii T**, **Arisawa A**, **Tamura T**. 2007. Crystal structure of cytochrome P450 MoxA from *Nonomuraea recticatena* (CYP105). Biochem. Biophys. Res. Commun. **361**:876–882.

61. **Stassi D**, **Donadio S**, **Staver MJ**, **Katz L**. 1993. Identification of a *Saccharopolyspora erythraea* gene required for the final hydroxylation step in erythromycin biosynthesis. J. Bacteriol. **175**:182–189.

62. **Clevenger KD**, **Bok JW**, **Ye R**, **Miley GP**, **Verdan MH**, **Velk T**, **Chen C**, **Yang K**, **Robey MT**, **Gao P**, **Lamprecht M**, **Thomas PM**, **Islam MN**, **Palmer JM**, **Wu CC**, **Keller NP**, **Kelleher NL**. 2017. A scalable platform to identify fungal secondary metabolites and their gene clusters. Nat Chem Biol **13**:895–901.

63. **Chen S**, **Wang J**, **Lin X**, **Zhao B**, **Wei X**, **Li G**, **Kaliaperumal K**, **Liao S**, **Yang B**, **Zhou X**, **Liu J**, **Xu S**, **Liu Y**. 2016. Chrysamides A–C, three dimeric nitrophenyl trans-epoxyamides produced by the deep-sea-derived fungus *Penicillium chrysogenum* SCSIO41001. Org. Lett. **18**:3650–3653.

64. **Kovacic P**, **Somanathan R**. 2014. Nitroaromatic compounds: Environmental toxicity, carcinogenicity, mutagenicity, therapy and mechanism. J. Appl. Toxicol. **34**:810–824.

65. **Keller NP**. 2015. Translating biosynthetic gene clusters into fungal armor and weaponry. Nat Chem Biol **11**:671–677.

66. **Macheleidt J**, **Mattern DJ**, **Fischer J**, **Netzker T**, **Weber J**, **Schroeckh V**, **Valiante V**, **Brakhage AA**. 2016. Regulation and role of fungal secondary metabolites. Annu. Rev. Genet. **50**:371–392.

67. **Janssen PH**, **Yates PS**, **Grinton BE**, **Taylor PM**, **Sait M**. 2002. Improved culturability of soil bacteria and isolation in pure culture of novel members of the divisions *Acidobacteria*, *Actinobacteria*, *Proteobacteria*, and *Verrucomicrobia*. Appl. Environ. Microbiol. **68** :2391–2396.

68. **Chen H**, **Walsh CT**. 2001. Coumarin formation in novobiocin biosynthesis: β-hydroxylation of the aminoacyl enzyme tyrosyl-S-NovH by a cytochrome P450 NovI. Chem. Biol. **8**:301–312.

69. **Ninnemann H**, **Maier J**. 1996. Indications for the occurrence of nitric oxide synthases in fungi and plants and the involvement in photoconidiation of *Neurospora crassa*. Photochem. Photobiol. **64**:393–398.

70. **Samalova M**, **Johnson J**, **Illes M**, **Kelly S**, **Fricker M**, **Gurr S**. 2013. Nitric oxide generated by the rice blast fungus *Magnaporthe oryzae* drives plant infection. New Phytol. **197**:207–222.

71. **Spatafora JW**, **Chang Y**, **Benny GL**, **Lazarus K**, **Smith ME**, **Berbee ML**, **Bonito G**, **Corradi N**, **Grigoriev I**, **Gryganskyi A**, **James TY**, **O'Donnell K**, **Roberson RW**, **Taylor TN**, **Uehling J**, **Vilgalys R**, **White MM**, **Stajich JE**. 2016. A phylum-level phylogenetic classification of zygomycete fungi based on genome-scale data. Mycol. **108** :1028–1046.

855 72. **Weathers PJ**. 1984. N_2O evolution by green algae. Appl. Environ. Microbiol. **48**:1251–
856 1253.
857

858 73. **Guieysse B**, **Plouviez M**, **Coilhac M**, **Cazali L**. 2013. Nitrous oxide (N_2O) production in
859 axenic *Chlorella vulgaris* microalgae cultures: evidence, putative pathways, and potential
860 environmental impacts. Biogeosciences **10**:6737–6746.
861

862 74. **Plouviez M**, **Wheeler D**, **Shilton A**, **Packer MA**, **McLenachan PA**, **Sanz-Luque E**,
863 **Ocana-Calahorro F**, **Fernandez E**, **Guieysse B**. 2017. The biosynthesis of nitrous oxide
864 in the green alga *Chlamydomonas reinhardtii*. Plant J.
865

866 75. **Philippot L**. 2005. Denitrification in pathogenic bacteria: for better or worst? Trends
867 Microbiol. **13**:191–192.
868

869 76. **Myburg AA**, **den Berg N**, **Viljoen A**. 2013. Pathogenicity associated genes in *Fusarium*
870 *oxysporum* f. sp. *cubense* race 4. S. Afr. J. Sci. **109**:1–10.
871

872 77. **McFadden HG**, **Wilson IW**, **Chapple RM**, **Dowd C**. 2006. Fusarium wilt (*Fusarium*
873 *oxysporum* f. sp. *vasinfectum*) genes expressed during infection of cotton (*Gossypium*
874 *hirsutum*)†. Mol. Plant Pathol. **7**:87–101.
875

876 78. **Jones CM**, **Welsh A**, **Throbäck IN**, **Dörsch P**, **Bakken LR**, **Hallin S**. 2011. Phenotypic
877 and genotypic heterogeneity among closely related soil-borne N_2- and N_2O-producing
878 *Bacillus* isolates harboring the *nosZ* gene. FEMS Microbiol. Ecol. **76**:541–52.
879

880 79. **Graf DRH**, **Jones CM**, **Hallin S**. 2014. Intergenomic comparisons highlight modularity
881 of the denitrification pathway and underpin the importance of community structure for
882 N_2O emissions. PLoS One **9**.
883

884 80. **Philippot L**. 2002. Denitrifying genes in bacterial and archaeal genomes. Biochim.
885 Biophys. Acta - Gene Struct. Expr. **1577**:355–376.
886

887 81. **Simão FA**, **Waterhouse RM**, **Ioannidis P**, **Kriventseva E V**, **Zdobnov EM**. 2015.
888 BUSCO: assessing genome assembly and annotation completeness with single-copy
889 orthologs. Bioinformatics **31**:3210–3212.
890

891 82. **She R**, **Chu JS-C**, **Uyar B**, **Wang J**, **Wang K**, **Chen N**. 2011. genBlastG: using BLAST
892 searches to build homologous gene models. Bioinforma. **27** :2141–2143.
893

83. **Altschul SF**, **Gish W**, **Miller W**, **Myers EW**, **Lipman DJ**. 1990. Basic local alignment search tool. J. Mol. Biol. **215**:403–410.

84. **Li W**, **Cowley A**, **Uludag M**, **Gur T**, **McWilliam H**, **Squizzato S**, **Park YM**, **Buso N**, **Lopez R**. 2015. The EMBL-EBI bioinformatics web and programmatic tools framework. Nucleic Acids Res. **43**:W580–W584.

85. **Mistry J**, **Bateman A**, **Finn RD**. 2007. Predicting active site residue annotations in the Pfam database. BMC Bioinformatics **8**:298.

86. **Finn RD**, **Mistry J**, **Tate J**, **Coggill P**, **Heger A**, **Pollington JE**, **Gavin OL**, **Gunasekaran P**, **Ceric G**, **Forslund K**, **Holm L**, **Sonnhammer ELL**, **Eddy SR**, **Bateman A**. 2010. The Pfam protein families database . Nucleic Acids Res. **38** :D211–D222.

87. 2015. UniProt: a hub for protein information. Nucleic Acids Res. **43**:D204–D212.

88. **Fish J**, **Chai B**, **Wang Q**, **Sun Y**, **Brown CT**, **Tiedje J**, **Cole J**. 2013. FunGene: the functional gene pipeline and repository. Front. Microbiol. **4**:291.

89. **Pruitt KD**, **Tatusova T**, **Maglott DR**. 2007. NCBI reference sequences (RefSeq): a curated non-redundant sequence database of genomes, transcripts and proteins. Nucleic Acids Res. **35** :D61–D65.

90. **Korf I**. 2004. Gene finding in novel genomes. BMC Bioinformatics **5**:59.

91. **Inglis D**, **Binkley J**, **Skrzypek M**, **Arnaud M**, **Cerqueira G**, **Shah P**, **Wymore F**, **Wortman J**, **Sherlock G**. 2013. Comprehensive annotation of secondary metabolite biosynthetic genes and gene clusters of *Aspergillus nidulans*, *A. fumigatus*, *A. niger* and *A. oryzae*. BMC Microbiol. **13**:91.

92. **Eddy SR**. 2009. A new generation of homology search tools based on probabilistic inference. Genome Inform. **23**:205–211.

93. **Powell S**, **Szklarczyk D**, **Trachana K**, **Roth A**, **Kuhn M**, **Muller J**, **Arnold R**, **Rattei T**, **Letunic I**, **Doerks T**, **Jensen LJ**, **von Mering C**, **Bork P**. 2012. eggNOG v3.0: orthologous groups covering 1133 organisms at 41 different taxonomic ranges. Nucleic Acids Res. **40**:D284–D289.

94. **Emms DM**, **Kelly S**. 2015. OrthoFinder: solving fundamental biases in whole genome comparisons dramatically improves orthogroup inference accuracy. Genome Biol. **16**:1–14.

95. **Richter M**, **Rosselló-Móra R**. 2009. Shifting the genomic gold standard for the prokaryotic species definition. Proc. Natl. Acad. Sci. **106** :19126–19131.

96. **Kurtz S**, **Phillippy A**, **Delcher AL**, **Smoot M**, **Shumway M**, **Antonescu C**, **Salzberg SL**. 2004. Versatile and open software for comparing large genomes. Genome Biol. **5**:R12.

97. **Hunter JD**. 2007. Matplotlib: A 2D graphics environment. Comput. Sci. Eng. **9**:90–95.

98. **Katoh K**, **Asimenos G**, **Toh H**. 2009. Multiple alignment of DNA sequences with MAFFT. Methods Mol. Biol. **537**:39–64.

99. **Price MN**, **Dehal PS**, **Arkin AP**. 2010. FastTree 2 – approximately maximum-likelihood trees for large alignments. PLoS One **5**:e9490.

100. **Mirarab S**, **Warnow T**. 2015. ASTRAL-II: coalescent-based species tree estimation with many hundreds of taxa and thousands of genes. Bioinformatics **31**:i44–i52.

101. **Waterhouse AM**, **Procter JB**, **Martin DMA**, **Clamp M**, **Barton GJ**. 2009. Jalview Version 2—a multiple sequence alignment editor and analysis workbench. Bioinforma. **25** :1189–1191.

102. **Galtier N**, **Gouy M**, **Gautier C**. 1996. SEAVIEW and PHYLO_WIN: two graphic tools for sequence alignment and molecular phylogeny. Comput. Appl. Biosci. **12**:543–548.

103. **Stamatakis A**. 2006. RAxML-VI-HPC: maximum likelihood-based phylogenetic analyses with thousands of taxa and mixed models. Bioinformatics **22**:2688–90.

104. **Ronquist F**, **Teslenko M**, **van der Mark P**, **Ayres DL**, **Darling A**, **Höhna S**, **Larget B**, **Liu L**, **Suchard MA**, **Huelsenbeck JP**. 2012. MrBayes 3.2: efficient bayesian phylogenetic inference and model choice across a large model space. Syst. Biol. **61**:539–542.

105. **Abascal F**, **Zardoya R**, **Posada D**. 2005. ProtTest: selection of best-fit models of protein evolution. Bioinforma. **21** :2104–2105.

106. **Posada D**. 2008. jModelTest: Phylogenetic model averaging. Mol. Biol. Evol. **25**:1253–1256.

107. **Pagel M**, **Meade A**, **Barker D**. 2004. Bayesian estimation of ancestral character states on phylogenies. Syst. Biol. **53**:673–684.

108. **Shimodaira H**, **Hasegawa M**. 2001. CONSEL: for assessing the confidence of phylogenetic tree selection. Bioinformatics **17**:1246–1247.

109. **Chen K**, **Durand D**, **Farach-Colton M**. 2000. NOTUNG: A program for dating gene duplications and optimizing gene family trees. J. Comput. Biol. **7**:429–447.

110. **Team RDC**. 2012. R: A language and environment for statistical computing. R Foundation for Statistical Computing, Vienna, Austria.

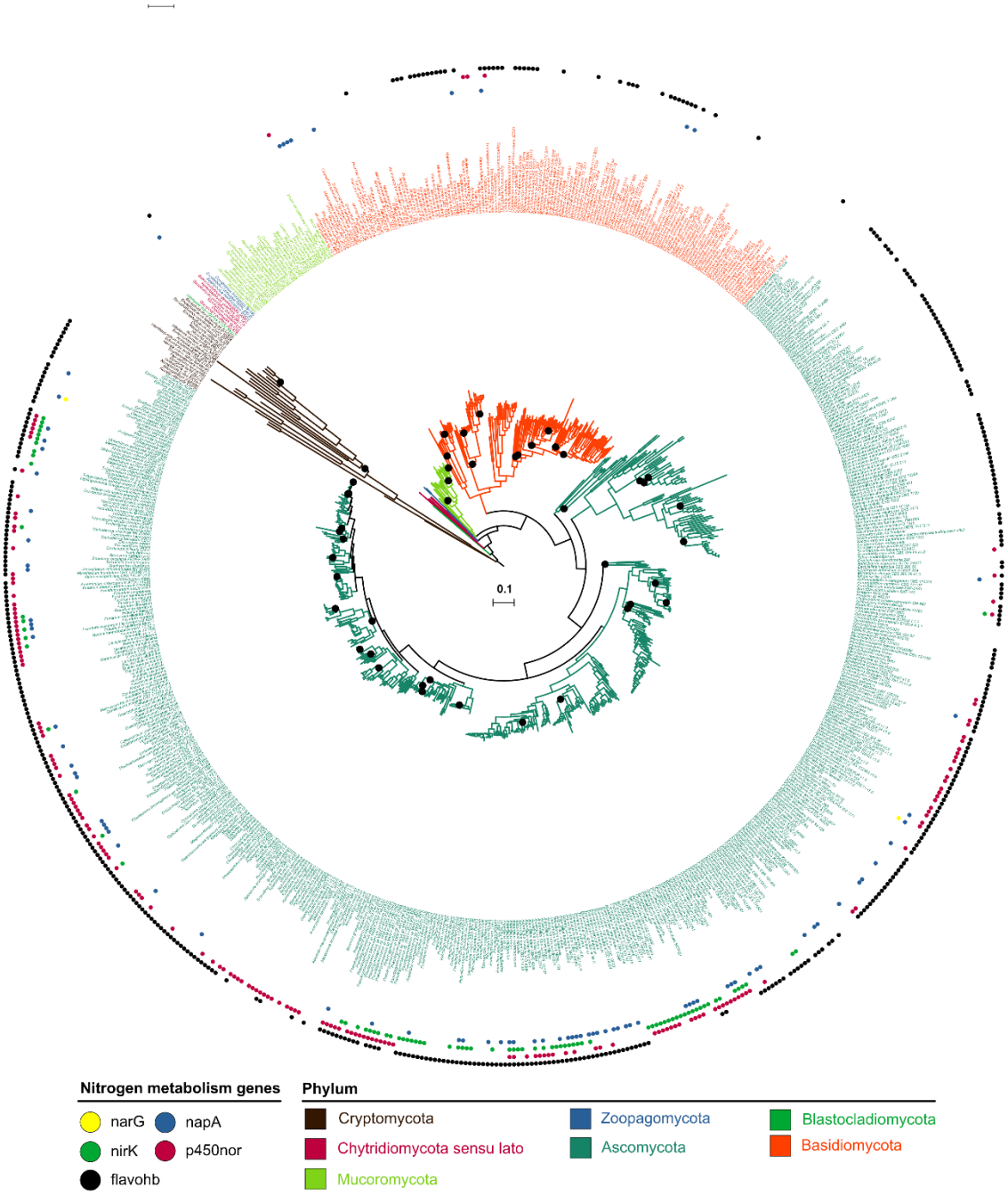

988

989 **Figure 1**. Maximum-Likelihood phylogeny of the kingdom Fungi inferred from a concatenated
990 alignment of 238 single copy marker gene amino acid sequences (see Materials and Methods).
991 Black circles marking branches indicate nodes with bootstrap percentages below 90%. Colored
992 markers outside taxon names specify the presence or absence of each gene (narG, napA, nirK,
993 p450nor, flavohemoglobin) within a fungal genome. Flavohb, flavohemiglobin genes involved in
994 NO detoxification. The scale bar (center of tree) represents amino acid substitutions per site. A
995 high-resolution file of the tree is available at https://doi.org/10.6084/m9.figshare.c.3845692.

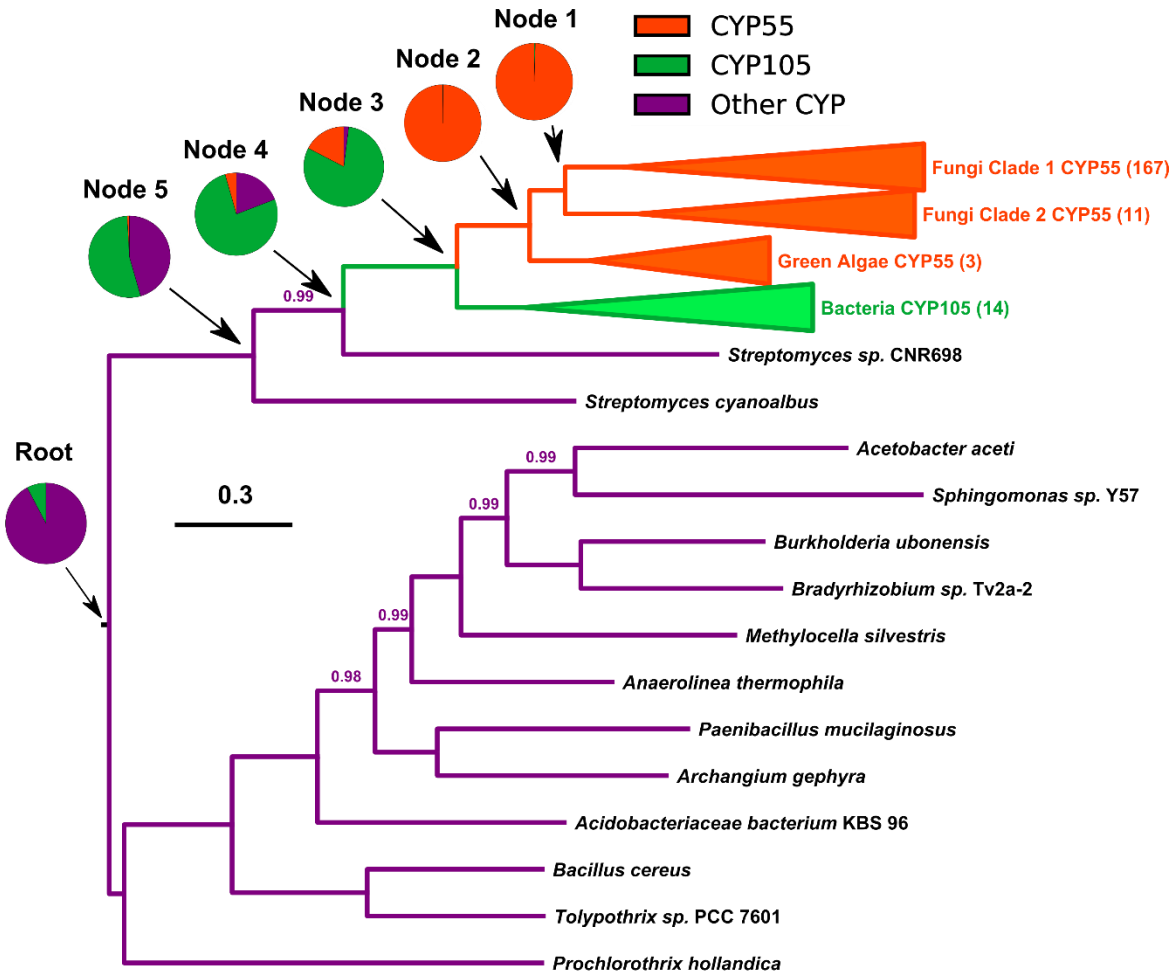

Figure 2. Midpoint-rooted Bayesian phylogeny of select families of cytochrome P450 amino acid sequences from fungi, algae, and bacteria. Ancestral state reconstruction was performed using CYP55 (orange), CYP105 (green), and other CYPs (purple) to uncover the shared ancestry of algal and fungal N_2O-producing cytochrome P450s with their most recent common bacterial ancestor. The scale bar indicates substitutions per site and posterior probability values < 1 are displayed above branches of the Bayesian MCMC analysis. Numbers in parentheses next to collapsed clades indicate the number of sequences in the clade. Values in pie charts are average probabilities of each character state across one representative Bayesian MCMC analysis.

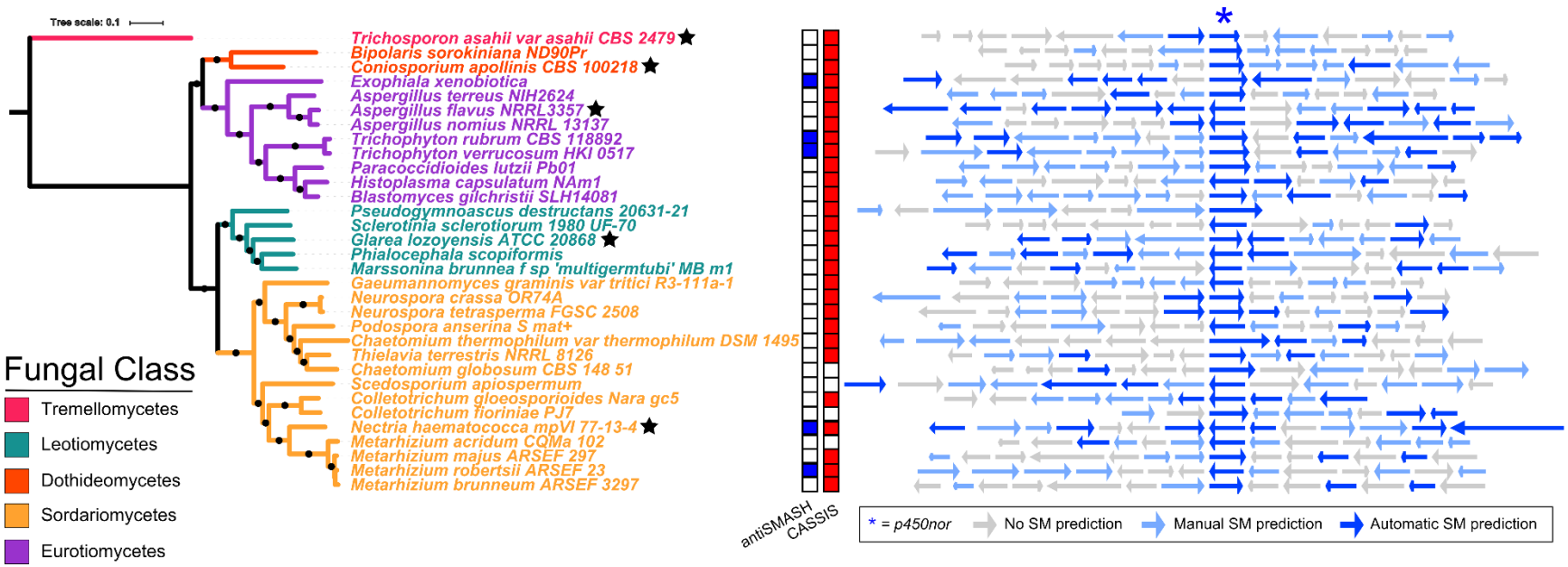

Figure 3. SM gene cluster predictions for a subset of 32 (167 total) *p450nor*-containing fungi. The boxes to the right of the rooted Maximum-Likelihood phylogeny indicate whether the *p450nor*-containing genomic region was predicted by antiSMASH (blue squares) or CASSIS (red squares) to be an SM gene cluster. White squares indicate no prediction. Colored arrows indicate protein-coding genes surrounding *p450nor* that were automatically predicted (dark blue arrow), manually predicted (light blue arrow) or not predicted (grey arrow) to be involved in SM (see Materials and Methods for details). The black stars next to species names are individuals chosen for in depth presentation of the genes surrounding *p450nor* (Fig. S9).

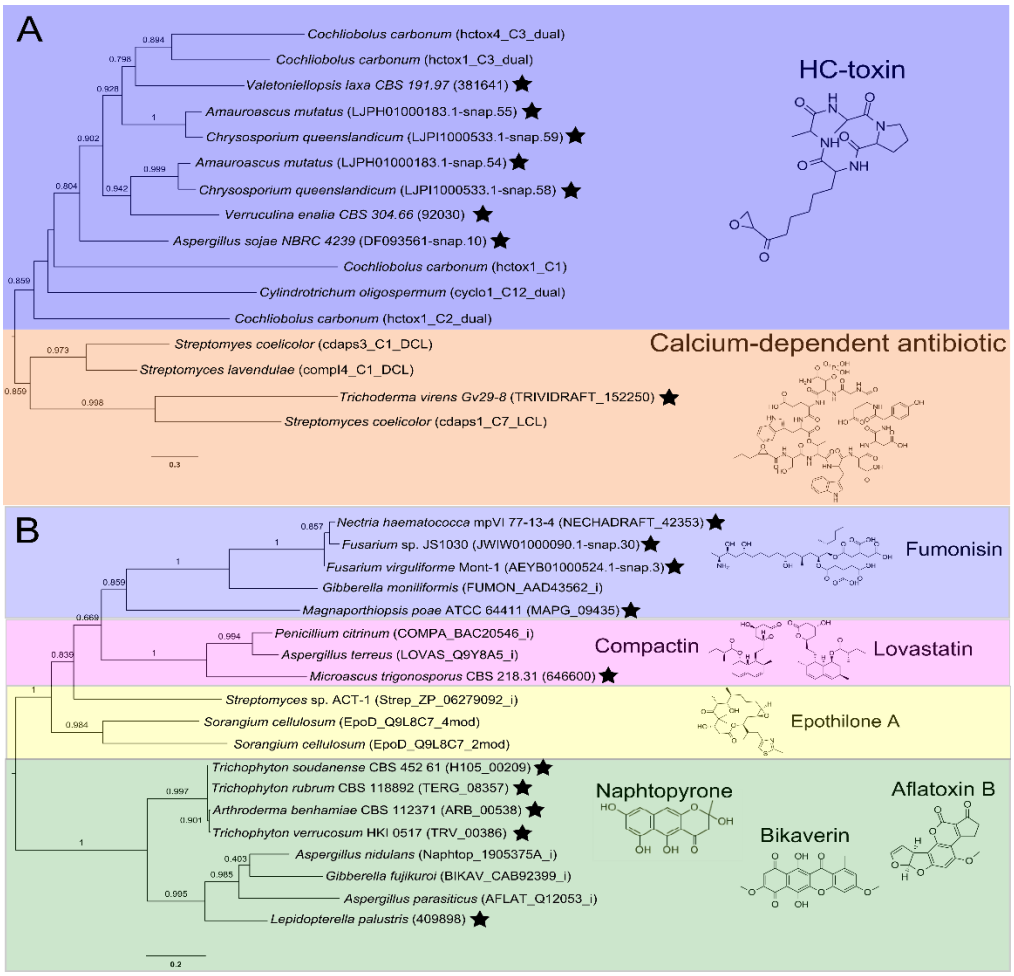

Figure 4. Maximum-Likelihood phylogenetic trees of non-ribosomal peptide synthase and polyketide synthase domains encoded within *p450nor*-containing genomic regions. Each phylogeny displays relationships of C-type condensation (C-type) (A) or ketosynthase (KS) domains (B) detected in non-ribosomal peptide and polyketide synthase amino acid sequences, respectively, encoded within *p450nor*-containing genomic regions. A black star next to taxa indicates C-type or KS domains identified in fungal genomes nearby *p450nor*. The NCBI or JGI accession numbers are shown in parentheses next to taxa with black stars. Taxa without black stars are reference amino acid sequences of C-type and KS domains curated by the NAPDOS database, and their NAPDOS accession numbers are indicated in parentheses. Proteins from species without accession numbers were predicted *ab initio* using SNAP (90) (see Materials and Methods for details). Chemical structures and names of secondary metabolites produced by NAPDOS reference sequences are indicated and highlighted distinct colors for clarity. Scale bars indicate amino acid substitutions per site. Values along branches indicate bootstrap support for the adjacent node.

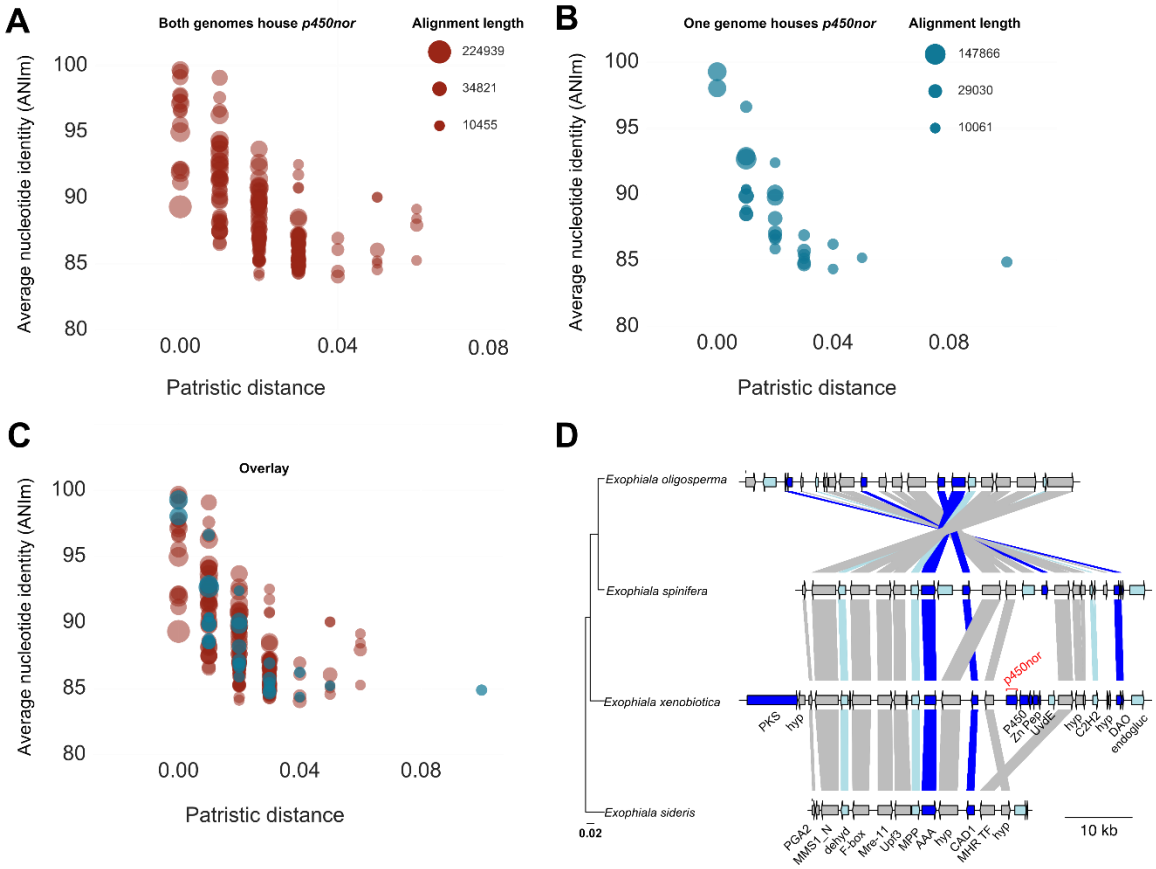

Figure 5. Within genera alignments of *p450nor*-containing genomic regions (N = 136) from species with and without *p450nor*. Alignment of two species with *p450nor*-containing genomic regions (red circles) (A) or between two species where only one member possesses *p450nor* (teal circles) (B). The overlay of the two plots in (C) indicates conservation of genomic architecture regardless of *p450nor* presence or absence. The size of the circles is proportional to the square root of the aligned length of the genomic regions. The gene synteny plot (D) highlights conservation of genomic architecture using a *p450nor*-containing genomic region from *Exophiala xenobiotia* aligned to three additional closely-related *Exophiala* species that do not possess *p450nor*. The arrows represent gene models within the gene region displayed. Both arrows and connecting lines above and below arrows are colored according to Figure 3 (see Materials and Methods for details). Lines connecting arrows between species indicate the genes are homologous. The scale bars (left to right) in (D) indicate substitutions per site and genome size in kilobases, respectively. The location of *p450nor* in *E. xenobiotica* is indicated in red font. The labels in black font describes the putative functions of proteins encoded by each gene. PKS - polyketide synthase, hyp – hypothetical protein, PGA2 – protein trafficking protein, MMS1_N – MMS1-like protein, dehyd – dehydrogenase, F-box – F-box domain containing protein, Mre-11 – double strand break repair protein Mre-11, Upf3 – nonsense mediated mRNA decay protein 3, MPP – metallophosphatase, AAA – ATPase, CAD1 – cinnamyl alcohol dehydrogenase, MHR TF – middle homology region transcription factor, P450 – cytochrome P450 reductase, Zn Pep – zinc peptidase superfamily protein, UvdE – UV-endonuclease, C2H2 – zinc finger C2H2 type, DAO – D-amino acid oxidase, endogluc – endoglucanase.

List of Supplemental Materials

Table S1. Counts of denitrification traits and their co-occurrences in fungal genomes.

Table S2. Results from approximately unbiased tests for the monophyly of fungal classes within *napA*, *nirK*, and *p450nor* gene trees. Where indicated, the monophyly of two lineages was also assessed. Bold font data indicate that the AU test rejected the monophyly of the taxa. Test significance was evaluated at $p \leq 0.05$.

Table S3. Results from species-tree gene-tree reconciliation using NOTUNG software for *napA*, *nirK*, and *p450nor* genes in fungi. Values are averages of solutions with standard deviations reported in parentheses.

Table S4. Predicted horizontal gene transfers of fungal *p450nor*, *napA*, and *nirK* genes based on alien index algorithm.

Table S5. List of genera containing species with and without *p450nor*.

Figure S1. Gene abundances of *narG*, *napA*, *nirK*, *p450nor*, and flavohemoglobins (colored bars) mapped on to fungal families (cladogram, left). Relationships among fungal families in the cladogram were derived from the NCBI taxonomy using the online tool phyloT (http://phylot.biobyte.de/index.html).

Figure S2. Maximum-Likelihood phylogenies connecting fungal species with their respective NO reductase (*p450nor*) gene sequence(s). On the left, an amino acid phylogeny of 238 concatenated single copy orthologues from fungal species in which one or more *p450nor* gene(s) were detected. The *p450nor* nucleotide phylogeny (right) demonstrates many instances of incongruence with the fungal species phylogeny. Black dots in each phylogeny represent bootstrap percentages greater than or equal to 90%. Scale bars represent amino acid (left tree) and nucleotide (right tree) substitutions per site. A high-resolution file of the tree is available at https://doi.org/10.6084/m9.figshare.c.3845692.

Figure S3. Cophylogenetic plot of *napA*-containing fungal species (left, N = 75) and the *napA* nucleotide tree (right, N = 78). Both are midpoint rooted Maximum-Likelihood trees where black dots represent bootstrap percentages ≥90 %. Scale bars indicate substitutions per site for the concatenated amino acid species phylogeny and nucleotide phylogeny, respectively. A high-resolution file of the tree is available at https://doi.org/10.6084/m9.figshare.c.3845692.

Figure S4. Cophylogenetic plot of *nirK*-containing fungal species (left, N = 82) and the *nirK* nucleotide tree (right, N = 83). Both are midpoint rooted Maximum-Likelihood trees where black dots represent bootstrap percentages ≥90 %. Scale bars indicate substitutions per site for the concatenated amino acid species phylogeny and nucleotide phylogeny, respectively. A high-resolution file of the tree is available at https://doi.org/10.6084/m9.figshare.c.3845692.

Figure S5. Plot of alien index values observed for *p450nor* genes (N = 178). Points above the hashed line at the origin are indicative of HGT. Names of fungal species with alien index values

above zero are ordered as their points appear on the graph. Thick horizontal lines represent the median alien index value. See Materials and Methods in the main text for details on alien index calculations.

Figure S6. Bayesian tree reconstruction of actinobacterial and proteobacterial 16S rRNA genes (left, N = 55) and cytochrome P450 family 105 amino acid sequences (right, N = 57). Both phylogenies represent 50% majority-rule consensus trees. The tree on the left is rooted with proteobacterial sequences as outgroup to the *Actinobacteria*. The tree on the right is midpoint rooted. Nodes with posterior probabilites ≥ 0.95 are indicated by black circles on an adjacent branch.

Figure S7. Midpoint rooted Bayesian (left) and Maximum-Likelihood phylogenies (right) of cytochrome P450 sequences (N = 408) demonstrating the affiliation of P450nor with other sequences belonging to members of the bacterial phyla Actinobacteria and Proteobacteria. Cyanobacterial cytochrome P450 sequences were included as outgroups. Black squares on branches (left tree) indicate ≥0.95 posterior probability or ≥90 % bootstrap replication (right tree). The colored legend indicates the cytochrome P450 family specified by shared amino acid identity of ≥40 % (D.R. Nelson, Hum Genomics 4:59-65, 2009).

Figure S8. Bayesian and Maximum-likelihood phylogenies of NapA, NirK, and P450nor amino acid sequence homologs extracted from the RefSeq protein database. A high-resolution file of these trees are available at https://doi.org/10.6084/m9.figshare.c.3845692.

Figure S9. Genome regions chosen for in depth presentation of protein coding genes surrounding *p450nor* in predicted BGC regions. Labels above genes are functional annotations from alignments to the eggNOG database. NCBI gene loci accessions are labeled below each gene.